SISSA

The new LUCID-2 detector for luminosity measurement and monitoring in ATLAS

To cite this article: G. Avoni *et al* 2018 *JINST* **13** P07017

View the article online for updates and enhancements.

Related content

IOP ebooks™

Bringing you innovative digital publishing with leading voices to create your essential collection of books in STEM research.

Start exploring the collection - download the first chapter of every title for free.

The new LUCID-2 detector for luminosity measurement and monitoring in ATLAS

G. Avoni,[b,c] **M. Bruschi,**[b] **G. Cabras,**[b,c] **D. Caforio,**[f] **N. Dehghanian,**[a] **A. Floderus,**[e]
B. Giacobbe,[b] **F. Giannuzzi,**[b,c] **F. Giorgi,**[b,c] **P. Grafström,**[b,c,1] **V. Hedberg,**[e]
F. Lasagni Manghi,[b,c] **S. Meneghini,**[b,c] **J. Pinfold,**[a] **E.Richards,**[d] **C. Sbarra,**[b] **N. Semprini**
Cesari,[b,c] **A. Sbrizzi,**[b] **R. Soluk,**[a] **G. Ucchielli,**[b,c] **S. Valentinetti,**[b,c] **O. Viazlo,**[d] **M. Villa,**[b.c]
C. Vittori,[b,c] **R.Vuillermet**[d] **and A. Zoccoli**[b,c]

[a]*Department of Physics, University of Alberta,*
  116 St & 85 Ave, Edmonton, AB T6G 2R3, Canada

[b]*INFN Sezione di Bologna,*
  viale C. Berti Pichat, 6/2, 40127 Bologna, Italy

[c]*Dipartimento di Fisica, Università di Bologna,*
  viale C. Berti Pichat, 6/2, 40127 Bologna, Italy

[d]*CERN,*
  CH-1211 Geneva 23, Switzerland

[e]*Department of Phyisics, University of Lund,*
  Professorsgatan 1, Lund, Sweden

[f]*Institute of Experimental and Applied Physics, Czech Technical University in Prague,*
  Horská 3a/22, 128 00 Praha 2, Czech Republic

  E-mail: per.grafstrom@cern.ch

Abstract: The ATLAS luminosity monitor, LUCID (**LU**minosity **C**herenkov **I**ntegrating **D**etector), had to be upgraded for the second run of the LHC accelerator that started in spring 2015. The increased energy of the proton beams and the higher luminosity required a redesign of LUCID to cope with the more demanding conditions. The novelty of the LUCID-2 detector is that it uses the thin quartz windows of photomultipliers as Cherenkov medium and a small amounts of radioactive ^{207}Bi sources deposited on to these windows to monitor the gain stability of the photomultipliers. The result is a fast and accurate luminosity determination that can be kept stable during many months of data taking. LUCID-2 can also measure the luminosity accurately online for each of the up to 2808 colliding bunch pairs in the LHC. These bunch pairs are separated by only 25 ns and new electronics has been built that can count not only the number of pulses above threshold but also integrate the pulses.

---

[1]Corresponding author.

https://doi.org/10.1088/1748-0221/13/07/P07017

Contents

1 Introduction

A new luminosity detector for the ATLAS experiment [1] has been designed in 2013, installed in 2014 and commissioned in 2015. The detector is called LUCID-2 and consists of several small Cherenkov detectors for luminosity measurements and luminosity monitoring. The novelty of the LUCID-2 detector is that it uses the thin quartz windows of photomultipliers as Cherenkov medium and that it uses small amounts of radioactive ^{207}Bi sources deposited on to these windows to monitor the gain stability of the photomultipliers. The result is a fast and accurate luminosity determination that can be kept stable during many months of data taking.

A difficulty when measuring luminosity at the LHC is that there is typically more than one interaction taking place during every bunch crossing and thus a measurement of the luminosity at the LHC really consists of measuring the average number of interactions (μ) that takes place every time two bunches cross each other in the experiment. In 2011 there were at most 20 pp-interactions per bunch crossing but this number doubled in 2012 and doubled again in LHC Run 2.[1] Luminosity measurements at the LHC must therefore be working even at extremely large pile-up. The aim of the new LUCID-2 detector is to measure luminosity by not only counting hits (signals over threshold) in the detector but also by integrating the signals with Flash ADCs (FADCs). The advantage with the latter so-called charge integration method is that it can in principle work at the very high number of pp-interactions per bunch crossing expected in LHC Runs 2 and 3.

Some 2808 different colliding bunch pairs can be filled in the LHC and it is in many cases very useful or even essential to measure luminosity for each individual pair of colliding bunches [2, 3] making it another goal of LUCID. Moreover, LUCID-2 is the only detector in ATLAS that can measure luminosity for the individual bunches by charge integration. In order to get this many colliding bunches in the LHC it was necessary to reduce the bunch separation time from 50 ns to 25 ns in 2015. This was another challenge for the new LUCID project.

The LUCID-2 detector provided a luminosity measurement from the very first runs with stable beam collisions in 2015 and has since then been essential for all cross sections measurements in ATLAS at 13 TeV during Run 2.

In addition, LUCID-2 provides LHC with fast luminosity and beam background information (every 1-2 seconds). Fast luminosity feedback on such time scales is an essential element for beam optimization. In the future this will also allow the implementation of so-called luminosity-levelling. During the first part of each fill, LHC will keep μ constant to a level sustainable by the detectors by either acting on beam separation, beam crossing angle or beam size variations. This level is currently being kept at an average μ of 50, but bunch to bunch differences can easily reach to 40%. This strategy is aimed at maximizing the integral luminosity and keeping the peak luminosity and pile-up under control.

The paper is organized in the following way. In section 2 a general description of LUCID-2 is given and section 3 deals with some issues related to the construction and installation. Section 4 provides the background to the Monte-Carlo simulation that lead to the design of LUCID-2 and section 5 describes the new electronics. The calibration systems used to keep the gain variations under control are described in section 6 and section 7 deals with operational issues. An overview

---

[1]In the present LHC terminology Run 1 covers the period 2010-2013, Run 2 the period 2015-2018 and Run 3 the period 2020-2022.

of how LUCID-2 is used for luminosity measurements is given in section 8 and finally Section 9 contains some conclusions.

2   General description of LUCID-2 including the development from LUCID-1

The old LUCID-1 detectors that have been used during the years 2009–2013 surrounded the beam pipe on both sides of the interaction point and were made up of twenty 150 cm long Cherenkov detectors consisting of aluminum tubes with 14 mm diameter that pointed towards the interaction region [1]. This detector was designed with characteristics very similar to CLC, the luminometer which successfully operated in the CDF experiment at Fermilab [4]. The gas in the detector was C_4F_{10} and the Cherenkov light produced in the gas was collected at the back of the aluminum tubes in two ways. Sixteen of the aluminum tubes had photomultipliers with a 14 mm diameter directly attached to the back of the tubes and for four Cherenkov tubes the light was collected by optical quartz fibers and sent to a low radiation area where it was measured by photomultipliers.

The original LUCID-1 detector was designed to measure luminosity with a 5% precision up to a μ-value of about 7 but it provided a much more accurate measurement at higher μ-values. As the μ-value was increased to values above 20 in 2011 it was noted that small signals from secondary particles that went through only part of the gas volume would add up and give signals above the discriminator thresholds (so-called "migration"). The number of counts from the detector would then no longer perfectly follow Poisson statistics and this would spoil the luminosity calculation. It turned out, however, that particles going through only the 1.2 mm thick quartz window of the photomultipliers would create enough Cherenkov photons for a sizeable signal and that the signals from the window suffered less from the same migration problem. As a result the detectors were operated without gas for a large part of 2011 and for all of 2012. Cherenkov light was also produced in the quartz fiber bundles that were used to read out a subset of the channels but the hits from these fibers could not be used due to migration. However it was found out, as expected, that integrating the total charge led to linearity. This was the motivation to later introduce the charge integration method mentioned in the introduction.

The large particle density in the LUCID location meant that the anode current from the photomultipliers was twice as a high as the one recommended by the manufacturer. In 2012 it was observed that the photomultipliers were ageing, i.e., their gain was reduced with time. To correct for this ageing, LUCID-1 had a system to inject LED light via optical quartz fibers to the front of the Aluminum Cherenkov tubes. Small amounts of LED light was used to measure the single photon electron peak and this gave an accurate gain measurement, but when the luminosity got too high the measurement was spoiled because of background from activation of materials surrounding LUCID.

Another problem that showed up at high luminosity was that during the typical ATLAS luminosity measuring period (∼ 60 sec), called a Luminosity Block (LB), some LUCID luminosity algorithms had hits for every bunch crossing. This phenomena is normally called zero-starvation and the solution to this problem is to reduce the acceptance of the detector.

During the long LHC shutdown between 2013 and 2015 the ATLAS beam pipe and LUCID-1 had to be removed and the collaboration decided to upgrade the beam pipe in the LUCID region. The motivation for changing the material of the ATLAS beam pipe from stainless steel to aluminum was that this would give a smaller background in the muon detector and less activation of the

beampipe. However, simulations showed that for a detector, like LUCID, situated close to the beam pipe, the number of particles hitting the detector would substantially increase (see section 4).

It was decided to build a new LUCID-2 detector that could meet the challenges in 2015 and beyond [5]. Given the limitations mentioned above, the solution was to build a detector without gas and with smaller photomultipliers that were situated further away from the beam line. Moreover, in a development project with the Hamamatsu Company, new photomultipliers were developed where a part of the photocathode was masked off by an Aluminum layer inside the photomultiplier in order to further reduce their acceptance (see figure 1).
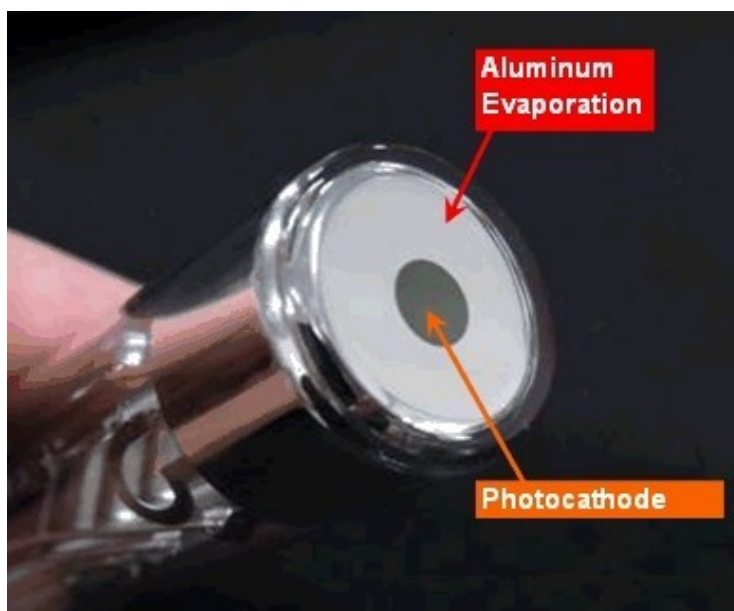

Figure 1. Photo of a modified Hamamatsu photomultiplier. The acceptance of the photocathode has been reduced by a thin aluminum layer on the window.

Figure 2 shows what one of the two LUCID-2 modules looked like in 2015. The two modules are called the A-side and C-side module following the ATLAS endcap naming convention.[2] It is a more compact design with 16 new smaller $\phi = 10$ mm diameter photomultipliers in each module arranged in 4 groups around the beampipe and with 4 bundles of quartz fibers read out by 4 additional photomultipliers situated some 1.5 m away from the detector inside the muon shielding. In this manner there is a total of $20 + 20 = 40$ photomultipliers in the two detector modules and they are read-out in such a way by the electronics that there are in total 5 different sub-detectors: the MODIFIED detector consists of $4 + 4$ photomultipliers with reduced acceptance ($\phi = 7$ mm); the LED detector has $4 + 4$ photomultipliers that are calibrated with LED signals while the $4 + 4$ BI detector is calibrated with ^{207}Bi sources; in addition there is a SPARE detector which is identical to the LED detector but not turned on; finally, the FIBER detector consists of $4 + 4$ quartz fiber bundles.

---

[2]In ATLAS, the positive x-axis points from the interaction point to the center of the LHC ring; the positive y-axis points upward to the surface of the earth. The detector half at positive z-values is referred to as the "A-side", the other half the "C-side".

The photomultipliers belonging to different sub-detectors are indicated in figures 2 and 3. A vital part of the detector is the relative calibration and gain monitoring systems that are using either LED signals or ^{207}Bi sources and this will be discussed in detail in section 6. During the data-taking in 2015 it became clear that the ^{207}Bi system was superior to the LED calibration system and the photomultipliers in the SPARE sub-detector were therefore equipped with ^{207}Bi at the start of 2016 and the LED and MODIFIED detectors were likewise equipped with ^{207}Bi at the start of 2017 (see figure 3).
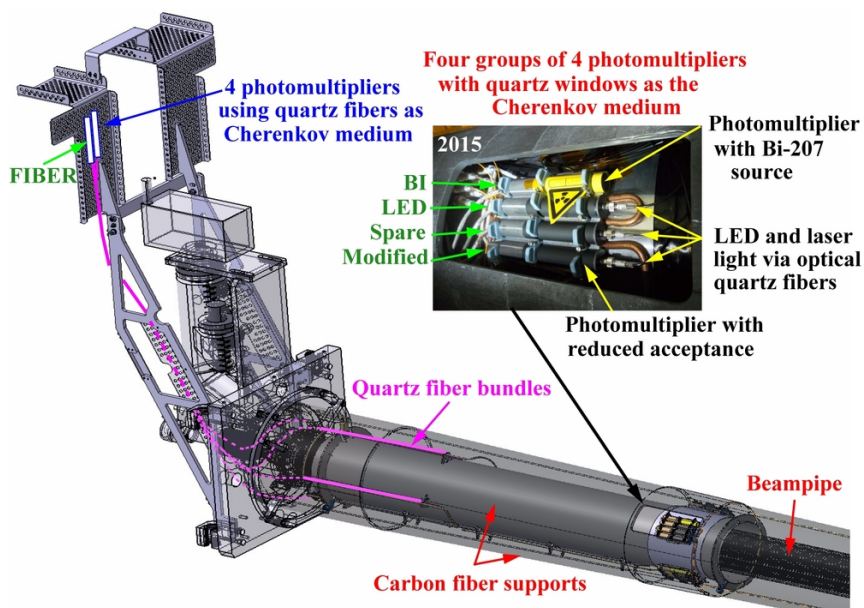

Figure 2. The new LUCID-2 detector during 2015.

The photomultipliers have been extensively tested with neutrons from reactors, radioactive sources, cosmics and by running them with large LED signals at a high rate for a long time. This testing has shown that the factor limiting their lifetime will be the charge collected and not radiation damage and this is the reason for keeping 4 + 4 of the photomultipliers in reserve. Radio Photo Luminescence (RPL) detectors were used to measure the radiation dose to the photomultipliers during 2012 and 2015. In 2012 the photomultipliers were exposed to 14 kGray and in 2015 to between 8.9 and 9.9 kGray.The photomultipliers were tested for up to 200 kGray without any adverse effects [5].

The LUCID-1 detector performance was affected by the stray magnetic field from both the ATLAS solenoid and the toroid. The photomultipliers in LUCID-2 are therefore all surrounded by magnetic shields made by so-called mu-metal (the black and yellow cylinders in the photo in figure 2). During the 2015 data-taking there was one period where the toroid magnets were turned off in order to align the ATLAS muon chambers with cosmics. The Bi-calibration runs taken before, during and after this period were used to study the effect of the toroid field on the LUCID photomultipliers. The gain of the four Bi-calibrated photomultipliers on the A-side increased on average by 0.9% when the toroid was turned off and decreased by 0.5% when the toroid was turned back on again. Thus it is clear that if there is an influence of the magnetic fields it is below the

% level and that LUCID-2 provides an accurate luminosity measurement also when the ATLAS magnets are turned off.

3   Construction

3.1   Mechanical design

The beam pipe in the region where LUCID is situated, is supported by a long cone which is attached at the back to an aluminum plate that in turn hangs off a solid shielding cylinder made of cast iron. This cone was originally made of aluminum but it was decided to change the cone material to carbon fibers to reduce background and activation further. Since completely new beampipes and support cones were designed it was possible to incorporate new features in the design, such as windows, that made it easier to support and provide access to LUCID. Figure 2 shows an overview of LUCID, the beam pipe and the support cone and figure 3 shows details of the various parts. LUCID consists mainly of a 1550 mm long support cylinder that is made of carbon fibers like the beam pipe support cone. The cylinder has a 1.5 mm thick wall and an outer diameter of 223 mm. The LUCID support cylinder is attached to the beam pipe support cone at its front and back in three points. At the back of the support cylinder four bundles of optical quartz fibers housed in aluminum tubes are attached to copper tubes that cool the fibers with water when the beam pipe is baked-out. In addition, 16 photomultipliers are attached to four aluminum supports sitting around a 1.5 mm thick cooling cylinder, as shown in figure 3. These aluminum supports can also be cooled down by water during beam pipe bake-out. Temperature probes are attached to the sides of the supports so that the temperature can be monitored. One of the aluminum supports is shown in the photo in figure 4 before being attached to the cooling cylinder. The photo shows how two spring-loaded blue attachment pieces hold the mu-metal cylinder and the base of a photomultiplier in place. This mu-metal cylinder has a wall thickness of 0.85 mm and it protects the photomultiplier from stray magnetic fields. At the front of the photomultiplier and its mu-metal cylinder, a cap made of PEEK[3] can be attached with a connector for optical quartz fibers that can transmit LED or laser light. The center of the photomultipliers sits at a distance of 125.5 mm from the beam line and 16.97 m way from the interaction point. This means that the pseudo rapidity coverage of the photomultiplier windows is between 5.561 and 5.641.

3.2   Installation

The installation of the LUCID detector (without photomultipliers) into the beam pipe support cone was not difficult, while the installation of the beam pipe into the LUCID cylinder and the support cone was more challenging and had to be done vertically as shown in figure 5. The whole assembly consisting of LUCID, the beam pipe and their supports with services was then installed in ATLAS as shown in figure 6. The assembly was hanged off the shielding that protrudes through the muon detectors to the left in the photo. After the assembly had been done the photomultipliers could be installed through the holes in the wall of the beam pipe support cone (see figure 2).

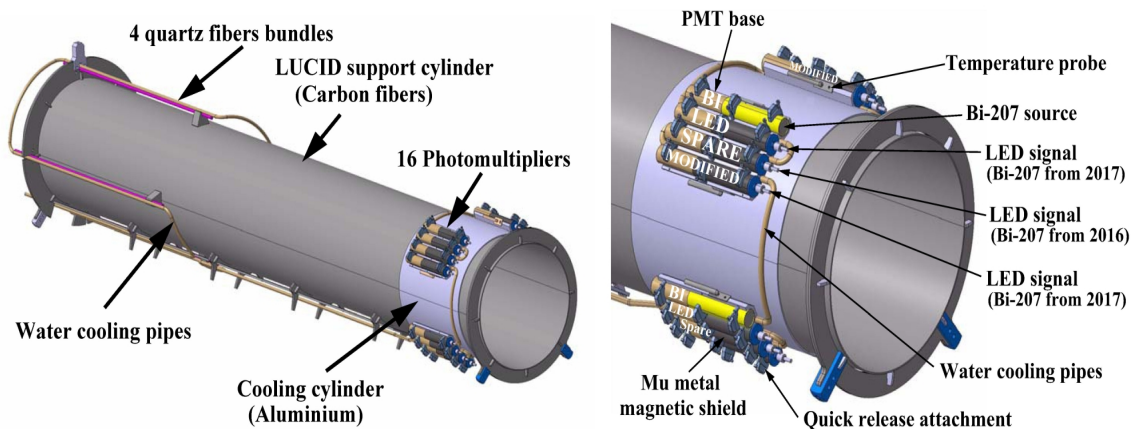[3]Polyether Ether Ketone with 30% Carbon.

Figure 3. The left drawing shows the LUCID support cylinder with the four quartz bundles at the back and the 16 photomultipliers at the front. The right drawing shows the support and cooling structure of the photomultipliers.
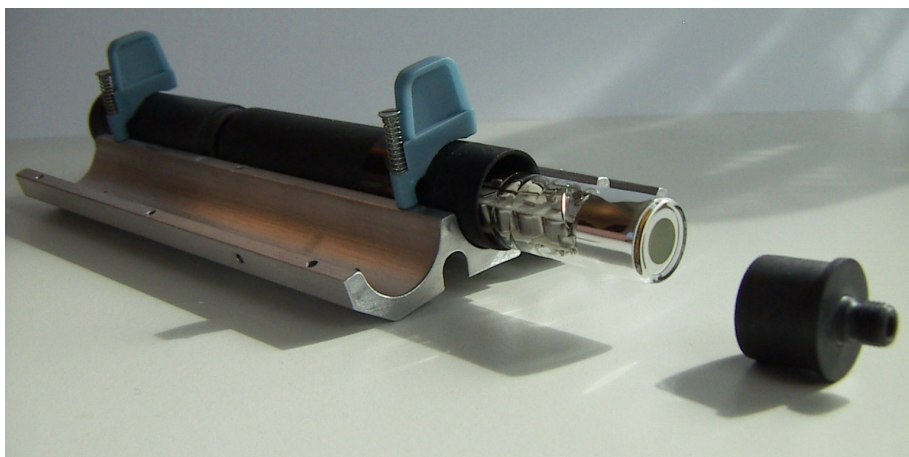
Figure 4. One of the aluminum cooling structures with a photomultiplier extracted from its mu-metal cylinder and its PEEK cap. The two plastic blue pieces on the top hold the photomultipliers in place on the detector. The cylinder containing the base is also seen at the back of the photo. The photomultiplier is of a special modified type where the acceptance of the window has been reduced.

3.3 Details on the ^{207}Bi sources

The gain monitoring system using ^{207}Bi is a unique part of the LUCID-2 detector. The reason why ^{207}Bi is a useful source for relative calibration is that in 11.5% of all disintegrations it emits internal conversions electrons with an energy of 482, 554, 566, 976, 1048 or 1060 keV and these energies are all above the Cherenkov threshold in quartz. However only electrons with an energy above 900 keV are expected to penetrate fully the quartz window without being stopped. It also sends out gammas mostly with an energy of 570 and 1064 keV but they are of no use for detector calibration. The half-life of ^{207}Bi is 33 years which means that the source will not change rate significantly during the detector lifetime. It turned out that it was not possible to obtain commercial closed sources of

Figure 5. The installation of the beampipe into LUCID and the support cone.
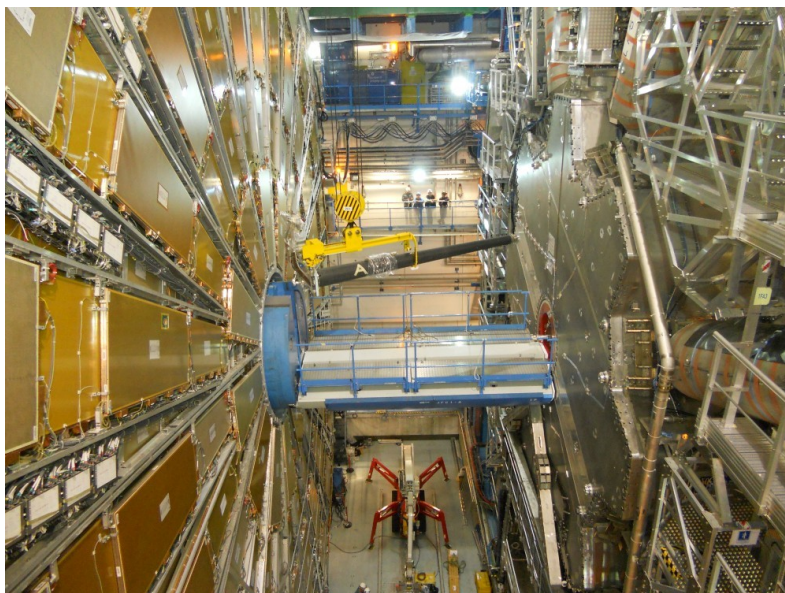

Figure 6. The installation of a LUCID-2 detector.

the right size and so open liquid ^{207}Bi sources were obtained from the Oak Ridge laboratory in the U.S.A. which have been used to produce sources with 20–40 kBq of ^{207}Bi for each photomultiplier. The application of the sources onto the photomultipliers was made at the radiological laboratory in Alberta University, Canada. The source is covered by a kapton tape and an aluminum foil but the main enclosure is provided by a radiation hard PEEK cap that is glued with radiation hard epoxy on to the photomultiplier as shown in figure 7.

A second enclosure is provided by the mu-metal cylinder. However, this cylinder is not glued to the photomultiplier in order to make it possible to carry out smear tests of the PEEK cap during shutdowns. PEEK has been chosen as a material for the cap since it is a semi-crystalline thermoplastic, very resistant to high temperatures and radiation. Smear tests done in 2016 and 2017 have not shown any sign of leakage of ^{207}Bi.

Figure 7. Photo of one of the Hamamatsu R760 photomultipliers with a ^{207}Bi source under the PEEK cap.

The procedure to apply the radioactive material on each photomultiplier was as follows:

- Approximately $10\,\mu l$ of ^{207}Bi solution was applied to a $25\,\mu m$ thick disc of aluminum foil using a micropipette;

- 24 hours were allowed for the solution to dry. Leaving roughly $20\,ng$ of ^{207}Bi on each foil as a salt deposit;

- The PMT was placed vertically, window up, inside a fume hood in the University of Alberta radiation laboratory and the aluminum disc was placed on top of the PMT window;

- A disc of kapton tape ($62\,\mu m$ thick with $25\,\mu m$ of silicone adhesive) was applied over the aluminum foil and the window of the PMT as a protective layer to initially secure the source material;

- Each PMT was placed in a light-tight aluminum tube and a rate test was performed in order to confirm that enough activity had been applied to the PMT;

- The PEEK caps were finally glued with epoxy glue over the end of the PMTs to seal the sources completely.

Two photomultipliers had the liquid ^{207}Bi applied directly to the PMT window. The pulseheight spectrum from these photomultipliers had a large component of pulses with a small pulseheight. The motivation for the aluminum foil is therefore to clean up the signal and to avoid low energy electrons reaching the photomultiplier window.

The photomultipliers attachment system that consists of spring-loaded pieces made of radiation hard Accura Bluestone[4] makes it possible to change a photomultiplier within a couple of minutes without tools. This is important since this region in ATLAS, close to the beam pipe and close to the so called TAS collimator, is one of the most radioactive areas of the experiment.

---

[4]Accura Bluestone is a rigid nanocomposite material used in 3D-printing which is a trademark of 3D Systems Inc.

4 Monte Carlo simulations

4.1 Introduction

This section is devoted to the Monte Carlo simulations used to upgrade the design of the LUCID detector from Run 1 to Run 2. The inelastic proton collisions are generated with Pythia6 [6] and the ATLAS detector response is modeled with GEANT4 [7]. Figure 8 shows the simulated pulse-height spectrum of LUCID-1. A PMT is said to have a hit when the number of photoelectrons recorded in the event is larger than a given threshold. The value of the threshold is arbitrary but one would like to include the full signal peak shown in figure 8 and at the same time be well above the noise level. Therefore a threshold of 15 p.e. is indicatively a good choice. The threshold determines the detector event efficiency (ϵ) and some of the systematic effects, as it will be discussed later in the text.
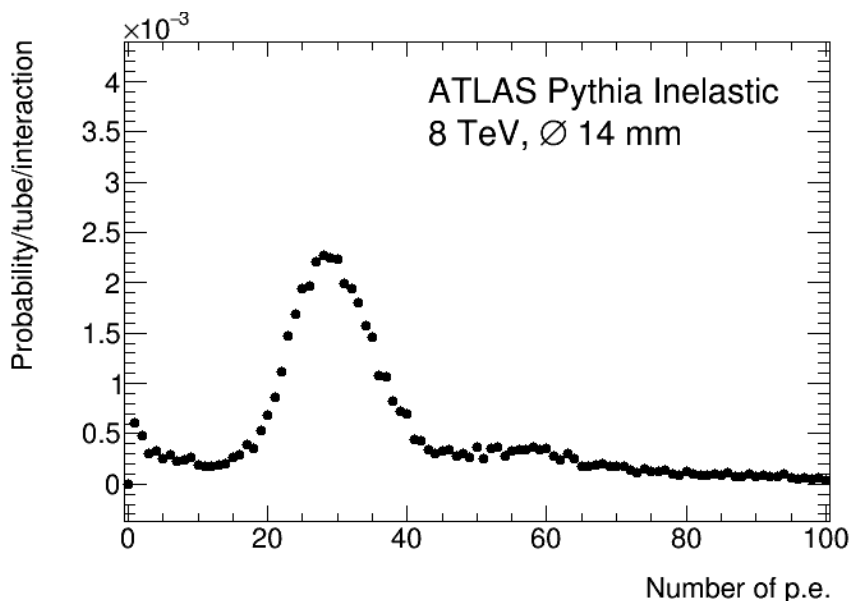

Figure 8. Simulated pulse-height spectrum of LUCID-1 and for a diameter of the PMT window of 14 mm.

Ideally the pulse-height spectra below threshold is empty and the probability to detect an event (P) can be expressed as a function of the average number of collisions per bunch crossing (μ):

$$P = 1 - e^{-\mu\epsilon} \tag{4.1}$$

Eq 4.1 can be used to measure μ and thus the luminosity. One can see that the probability to have an event becomes close to one when the product $\mu\epsilon$ is too large. This is called zero-starvation and imposes a limit on ϵ. The implications of zero-starvation for different μ-ranges are discussed more in detail in section 8.1.

4.2 From LUCID-1 to LUCID-2

LUCID-1 was, as mentioned previously, suffering from zero starvation towards the end of Run 1 (8 TeV) and this was expected to further increase in Run 2 (13 TeV) due to the increased pp cross section, as well as the change of beam pipe. Monte Carlo simulations were performed to estimate

those effects. Results are shown in table 1 where the expected variation of the LUCID-1 acceptance going from Run 1 to Run 2 is reported for some different PMT radii.

The table shows that the LUCID-1 acceptance was expected to increase from 60% to 80% from the combined effect of a larger center of mass energy and an aluminum beam pipe. One obvious way to reduce the geometrical acceptance of the detector was to use smaller PMT windows. In the table one can see that with a 10 mm window the acceptance is still higher than that of LUCID-1 while it becomes smaller by further reducing the size of the PMT window to 5 or 3 mm.

Table 1. The expected LUCID-1 acceptance for various scenarios from Run 1 to Run 2 for a detection with 16 + 16 tubes and a threshold 15 photoelectrons. For the simulation studies presented in this paper a Run 2 energy of 14 TeV was assumed while the actual Run 2 energy is so far 13 TeV. The term acceptance refers to the ϵ_{OR} efficiency, namely the probability to detect an event in either one or both LUCID detectors.

Energy [TeV]	ϵ_{OR} [%]	Comments
8	59.56 ± 0.16	LUCID-1
14	64.90 ± 0.15	LUCID-1
14	79.30 ± 0.50	Al-beam pipe
14	69.68 ± 0.07	PMT diameter 10 mm
14	36.59 ± 0.07	PMT diameter 5 mm
14	16.78 ± 0.05	PMT diameter 3 mm

In figure 9 the typical photoelectron distribution is shown, obtained from a PMT in single pp collisions (8 and 14 TeV) for some of the cases used in table 1.

A possibility to further reduce the acceptance for a given PMT is to reduce the number of tubes actively measuring the luminosity. Table 2 shows the values of the LUCID-2 acceptance for different number of tubes (14 TeV, 10 mm PMT windows).

Table 2. Dependence of the LUCID-2 acceptance on the numbers of tubes(14 TeV, 10 mm PMT windows).

Tubes/side	ϵ_{OR} [%]
16	69.68 ± 0.07
8	53.66 ± 0.07
4	37.71 ± 0.07
2	22.75 ± 0.06
1	13.14 ± 0.05

4.3 Signal migration

Eq. 4.1 is valid in the ideal case of a pulse-height spectra without small signals below threshold. Figure 8 shows that this is not the case. If the region below threshold gets filled by small signals, an additional increase of the hit probability as a function of μ can be expected. This is the so-called
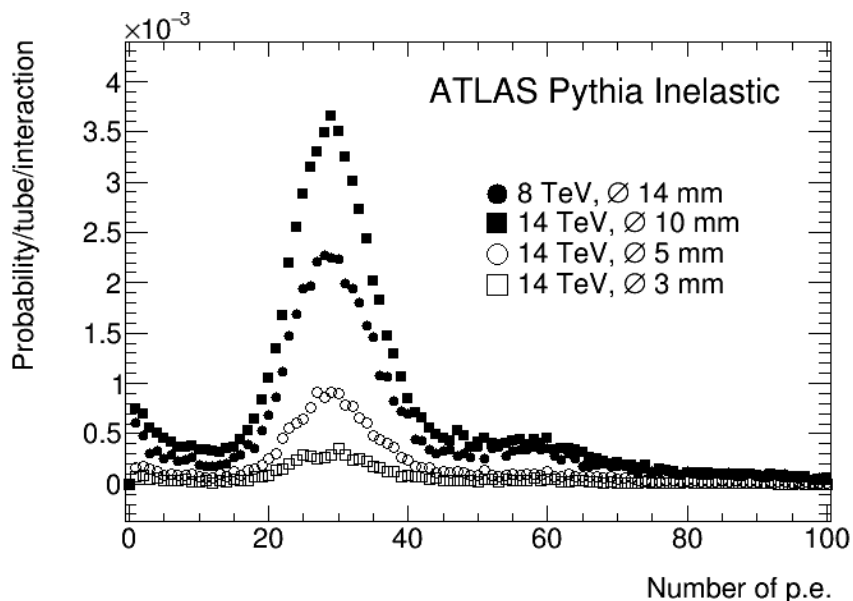
Figure 9. Typical photoelectron distribution obtained from a PMT in single pp collisions at different center of mass energies (8 and 14 TeV) and for different diameter of the PMT window (14 mm, 10 mm, 5 mm, 3 mm).

"signal migration", i.e. the overlap of several small signals below thresholds from different pp-interactions which add up to a large signal above threshold leading to a deviation from the Poisson assumption. Signal migration is not straightforward to predict analytically. An example of signal migration is illustrated in figure 10 where photoelectron spectra obtained with increasing values of μ with a 10 mm PMT window and 14 TeV center of mass energy are shown. The depletion of the region below threshold as a function of μ is an indication of potential systematic effects caused by signal migration.

4.4 Dependence of signal migration on the threshold

One can expect that the systematic effect due to signal migration is a function of the hit threshold. In the extreme case of a threshold at zero, no migration effect is expected. By increasing the threshold, the region below it gets more and more filled and therefore signal migration is expected to increase. How strongly the effect depends on the threshold position is not easy to predict. Figure 11 shows the expected fraction of events detected in LUCID as a function of μ for different values of the hit threshold. In this study one event is detected if at least one of the 16 + 16 tubes is hit. Values calculated according to the theoretical formula (Eq 4.1) are superimposed to each histogram as a continous line. Figure 11 shows that the deviation of the simulation from the calculated value increases with the threshold. The deviation is negligible for thresholds smaller than 15 photoelectrons.

4.5 Dependence of signal migration on the number of PMTs

In order to estimate the consequences in terms of signal migration when running the LUCID-2 detector with fewer tubes, the same study shown in figure 11 was repeated with the different
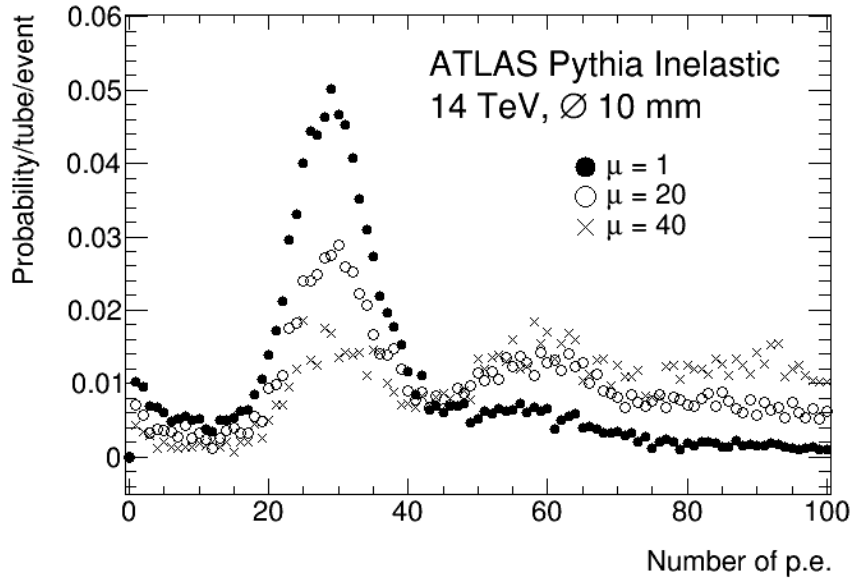
Figure 10. Photoelectron spectra for different pileup configurations (μ = 1, 20, 40) and for a diameter of the PMT window of 10 mm.
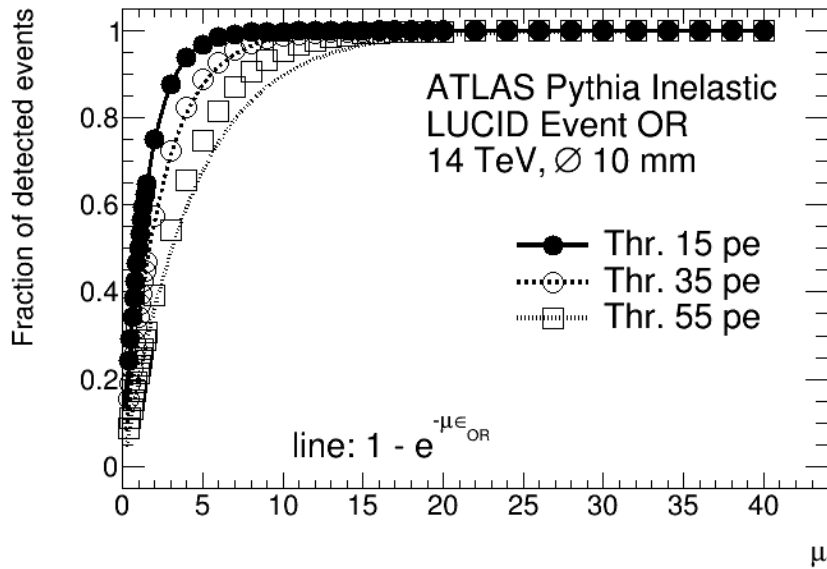

Figure 11. Fraction of events detected in LUCID as a function μ for different values of the hit threshold for a diameter of the PMT window of 10 mm. One event is detected if at least one of the 16 + 16 tubes is hit.

detector configurations reported in table 2. The results are shown in figure 12 where the fraction of events detected in LUCID as a function of μ is reported for different numbers of counting PMTs. Figure 12 shows that with a 10 mm window and a 15 photoelectron threshold the effect of signal migration is small for all number of tubes involved in the luminosity algorithm.
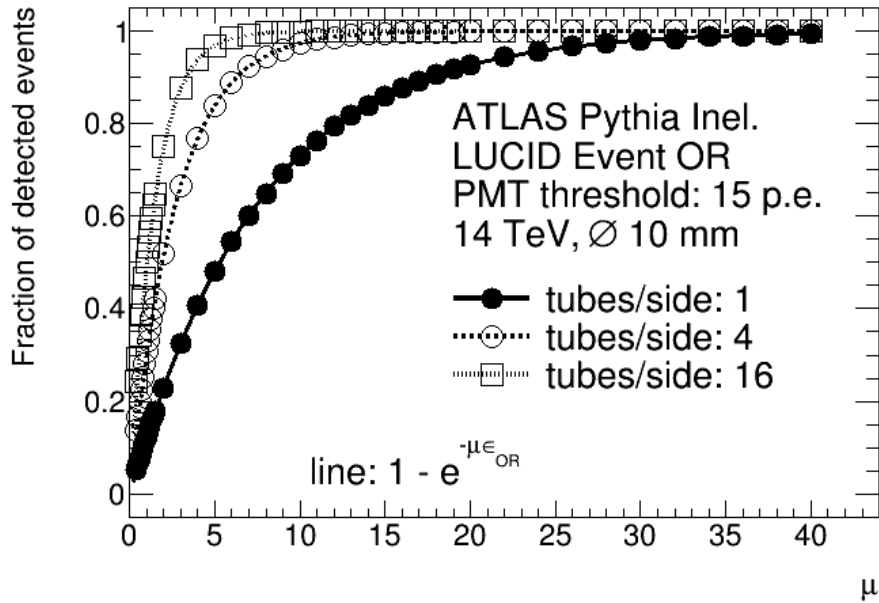
Figure 12. Fraction of events detected in LUCID as a function of μ for different numbers of counting PMTs and for a diameter of the PMT window of 10 mm. One event is detected if at least one of the 16 + 16 tubes is hit.

4.6 Signal migration in case of modified PMTs

The modified PMTs developed together with Hamamatsu were also simulated. Ideally, charged particles crossing the opaque region of the modified PMT should leave no signal. However, since the Cherenkov light is produced in a cone with an opening angle of 47 degrees, charged particles going through the opaque region can still have part of the light cone reaching the photocathode resulting in smaller photomultiplier signals.

This effect emphasizes edge effects normally present in standard PMTs. When the incident particle is sufficiently close to the border of the PMT window, a fraction of the light cone is reflected inside the window and can be lost if the photocathode does not cover the entire surface of the window.

Edge effects are confirmed by a MC simulation in which 180 GeV electrons impact perpendicularly on the window of the front face of standard and modified PMTs. The standard PMT is simulated with a 1.2 mm thick disc of quartz (bulk) in which Cherenkov photons are produced by the passage of charged particles with a sufficiently high energy. The side of the quartz disc facing the photocathode is equipped with a coaxial virtual disc capable of counting Cherenkov photons that simulates the photocathode (the sensitive area).The modified PMT is simulated by reducing the surface of the sensitive area, while keeping constant the diameter of the bulk to 10 mm.

The pulse-height spectra of a standard (10 mm) and modified PMTs (6 and 8 mm) obtained with perpendicular electrons impinging are shown in figure 13. Due to a larger edge effect, modified PMTs have a potentially larger migration effect and this was the reason why the detector was only partially equipped with this type of PMTs.
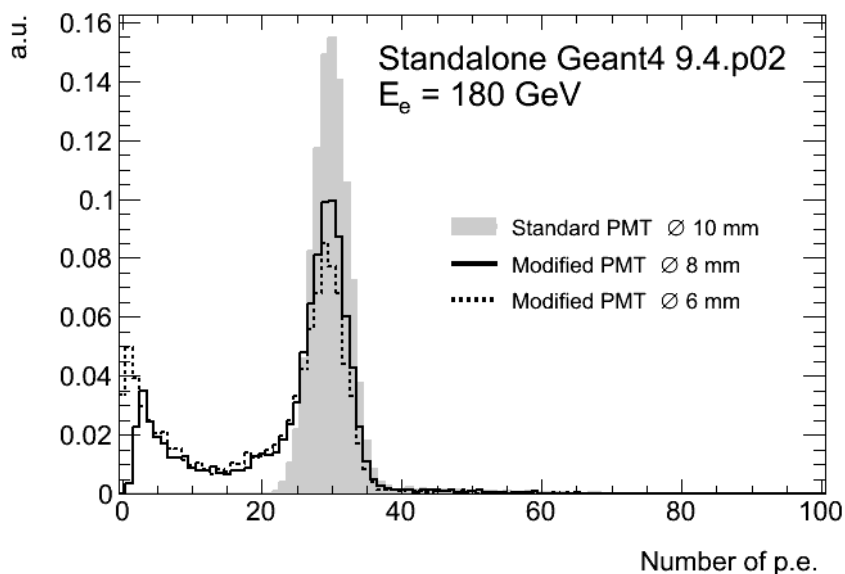
– 14 –

Figure 13. Pulse-height spectrum of a modified PMT (6 and 8 mm) superimposed to that of a standard PMT(10 mm).

4.7 Removing the gas radiator in LUCID-2

The LUCID-1 detector was equipped with 1.5 meter long Cherenkov gas tubes placed in front of the readout PMTs in order to increase the rate of photoelectrons per primary charged particle crossing the tubes along their axis. However, the presence of long and thin tubes was also increasing the rate of small signals due to secondary particles crossing the tubes transversally at large angles. This is illustrated in figure 14 where the simulated photoelectron spectra obtained with LUCID-1 in Run 1 (gas and PMT) are shown together with the separated contributions using only the PMT as radiator. In this case, the inelastic proton collisions are generated with Phojet 1.12 [8], the ATLAS detector response is modeled with GEANT3/GCALOR [9], with the exception of the LUCID detector which is modeled with GEANT4 [7].

The fraction of events below threshold is largely increased by adding up the contributions from the gas for two reasons: off-axis secondary particles give in average smaller light yields in the gas compared to the PMT and the probability of a secondary particle crossing the long tube is much larger compared to the thin PMT windows. In order to reduce the effect of signal migration, it was decided to remove the gas radiator in LUCID-2.

4.8 Summary

The design of the LUCID-2 detector was developed with the goal of reducing the detector acceptance compared to LUCID-1 and to minimize the systematic effects due to signal migration in the measurement of luminosity. Therefore it was decided to:

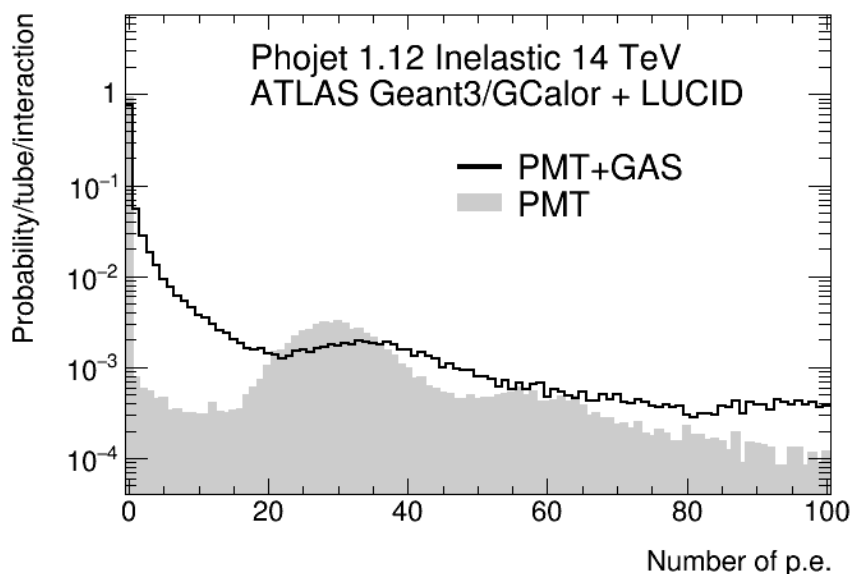- Remove the Cherenkov gas radiator and use only the PMT windows.

Figure 14. Simulated photoelectron spectra obtained with LUCID-1. The separated contributions of photoelectrons from Cherenkov light emissions in the PMT window and from the PMT window and the gas are superimposed.

- Divide the detector into five sub-detectors with 4 + 4 PMTs each instead of the 16 + 16 used in LUCID-1.

- Reduce the size of the PMT window from 14 mm to 10 mm and to 7 mm for one of the sub-detectors.

5 Electronics

A completely new electronics was developed for LUCID-2. The new electronics can count discriminator hits from the photomultipliers as in the past but in addition integrate the signals with FADCs. The advantage of a measurement of integrated pulses is that it is proportional to the number of particles going through the detector and it is therefore not affected by the already mentioned migration problem. Charge measurements can also be applied to fiber bundles not suitable for hit counting. On the other hand, charge integration algorithms are more sensitive to PMT gain variations, making the calibration procedure crucial.

The new electronics was placed close to the detectors in the experimental cavern in order to cope with 25 ns bunch separation time. With LUCID-1 the analog signals had to travel 100 m before they were digitized which meant that the signal width was larger than 25 ns when they reached the electronics. The LUCID-2 electronics is situated about 15 m away from the photomultipliers and the cables connecting the electronics with the photomultipliers are thick and fast high-performance cables so that the signals do not deteriorate before being digitized.

Figure 15 shows a block diagram of the electronics used for the LUCID-2 detectors. The photomultiplier pulses are fed to 4 LUCROD boards where signals are amplified, digitalized,

discriminated and integrated. Hit patterns corresponding to all possible bunch crossings (25 ns time slots) are transmitted to two custom VME boards (LUMAT boards) located about 100 m away, via optical links. As in LUCID-1, the LUMAT boards use hits to produce the counts needed by luminosity algorithms that uses signals from the two sides of the detector.
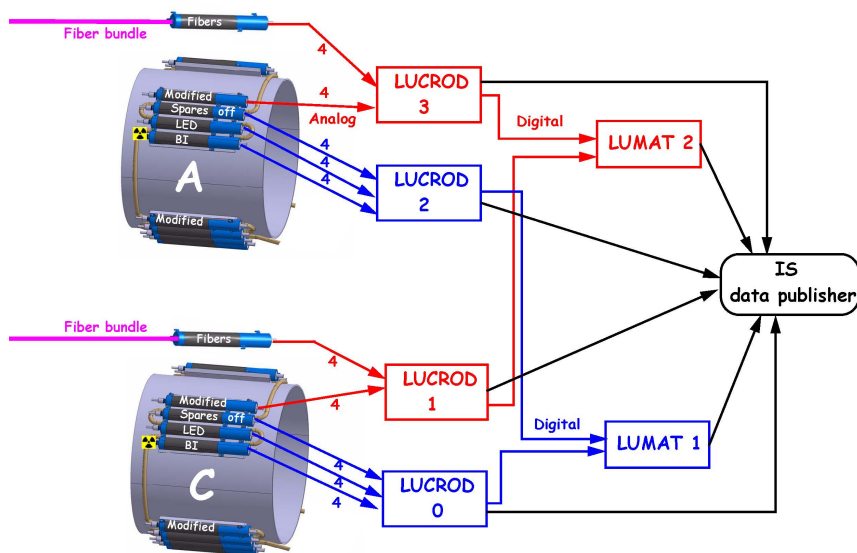

Figure 15. Block diagram of the electronics for the LUCID-2 detector.

The LUCROD board, a custom 9U VME board designed by the Electronics Lab of the Bologna Section of INFN, is shown schematically in figure 16 and a picture is shown in figure 17. The board features 16 lemo analog inputs, 16 lemo analog outputs (amplified copies of the inputs), four lemo digital I/O channels for triggering and debugging purposes, as well as JTAG and optical-link connectors. In additions, it holds a TTCrq[5] to receive external synchronization signals, and optical transceivers to deliver digital information. It operates with several internal clocks that can be aligned with the ATLAS 40 MHz main clock thanks to the TTCrq such as a 40 MHz clock, 320/480 MHz clocks used by the FADC, and a 50 MHz clock used by the transceiver and by their communication block.

Each LUCROD input is fitted with two independent and programmable amplifiers (with a gain of up to a factor of 16), one serving the analog output and the other one feeding a 320/480 MHz FADC[6] with 12-bit resolution (Equivalent Number of Bit $\simeq$ 10) and 1.5 V dynamic range. The zero level of the signals is adjustable with dedicated DACs.

Each LUCROD board hosts one group of eight channel FPGAs[7] and another group of two main FPGAs.[8] The former are directly connected to the inputs, each receiving the digitized data of two

---

[5]A mezzanine card developed by the CERN microelectronics group to handle Timing, Trigger and Control systems for the LHC (http://ttc.web.cern.ch/TTC/).

[6]AD9434BCPZ-500.

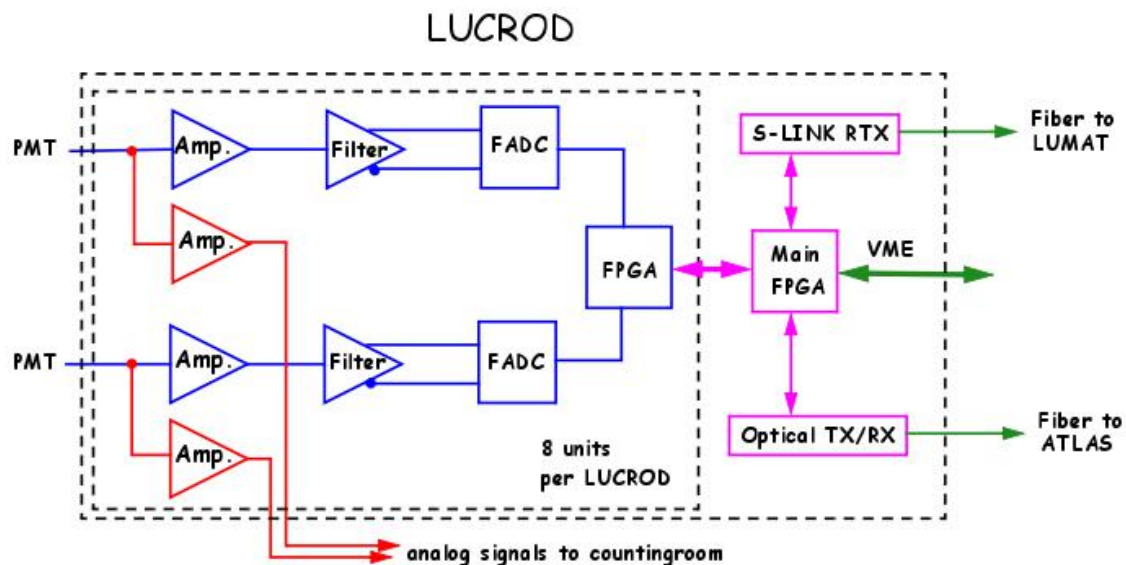[7]Altera Cyclone IV EP4CE40F484.

[8]EP4CGX30F484.

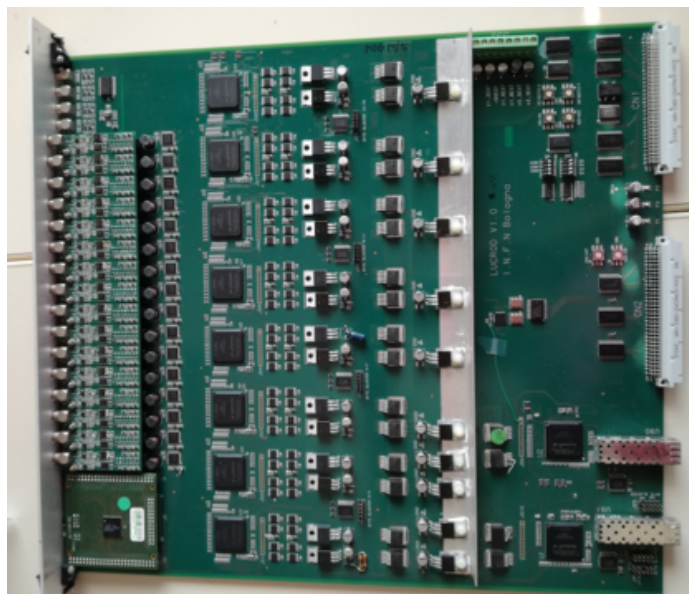**Figure 16**. Block diagram of the LUCROD board.

Figure 17. Picture of the LUCROD board.

channels. The latter provides the VME interfaces and the interface to the optical transceivers. All data buses are 16-bit, while the VME interface have both 16 and 32 bits.

In the channel FPGAs the digitized inputs are summed over each BCID (Bunch Crossing ID) period (25 ns, or 8 clock samples) to provide charge information, and the maximum pulseheight is compared to a programmable threshold to define hits within the same time windows. While hits and charge are accumulated in 3564-slot FIFOs (the depth corresponds to an LHC orbit), 64 samples of the digitized waveforms are made available for VME readout upon the presence of a trigger,

selectable between a programmable portion of the LHC orbit, or the presence of a hit. This slow VME readout provides a monitoring data stream with a hardware sampling of each PMT waveform. The main FPGAs receive charges and hits from programmable combinations of the channel FPGAs and provide charge-sums, hit-sums and event (at least one hit in one of the selected inputs) sums with BCID granularity. In addition the main FPGA routes hits to the output transceiver that feeds optical fibers connected to a LUMAT board. Since the transceiver operates at a 100 MHz frequency and sends serialized 16-bit words to the optical fiber, an interface is needed in the FPGA to implement an 8b/10b protocol and bridge the clock domains. This is accomplished through an elastic buffer where control k-words are added with the triple purpose of feeding the higher transceiver clock, serving as alignment word for the protocol and providing a reference to rebuild the 32-bit words out of the two 16-bit words sent through the transceiver. The hit pattern words sent from the LUCROD also contain an orbit signal that marks the beginning of the orbit (the Event Counter Reset signal received by the TTCrq) and an internally generated counter. These are used in the LUMAT board to align the side-A and side-C signals and to check for word loss.

Since the LUCROD boards are located close to the PMTs, in a zone that cannot be accessed during LHC running periods, a dedicated firmware was developed to allow for loading and changing the firmware itself, both via VME and via another VME board acting as a VME blaster. As described in section 7.2, this capability proved to be necessary in order to recover from Single Event Upset (SEU).

The LUMAT board is an evolution of the EDRO board described in ref. [10], with LUCID-dedicated firmware. In LUCID-1, the Edro Programmable Mezzanine Cards (EPMC), equipped with Altera Cyclone II FPGAs, received hits as LVDS signals generated by custom Constant Fraction Discriminator (CFD) VME boards located in the same electronics room as the LUMAT boards. In LUCID-2, since hits are generated nearby the detector, the initial EPMCs have been substituted by the FTK Input Mezzanines (FTK IM) [10], able to receive optical data from up to 4 S-link connections, containing both hits as well as synchronization data. The FTK IM, hosting two Spartan IV FPGAs, were programmed to receive two streams of hit data from two LUCROD boards dedicated to side A and C. The two streams of hits are then suitably synchronised before sending the hit data to the main FPGA of the LUMAT board, a Stratix II from Altera, where the main bunch-by-bunch luminosity algorithms are implemented.

Both the LUCROD and the LUMAT board cumulate hits and events (the LUCROD integrates charges as well) over LB periods, with BCID granularity, on internal FIFOs that are read via VME interface by the TDAQ software at the end of each integration period. A pair of FIFOs is needed for each integrated data. One is incremented while the other is read, without losses between FIFO switches. While the LUCROD board implements the evaluation of luminosity algorithms for single channels as well as OR on one side of ATLAS at a time, the LUMAT board, receiving hits from the two sides, performs luminosity algorithms that take advantage of the possible correlations among the two sides by counting, for example, the total number of hits in the two detectors or counting events where hits have been observed in both sides.

The cumulated data read at the end of each LB is made available for further elaboration by publication onto the Information Service (IS) [11, p. 161], a component of the ATLAS Online Software [11, pp. 6–9 and 23–31] that provides the means to share information between software applications in a distributed environment.

At present, the charge and hit algorithms are implemented individually for each input; for the same kind of sensors single side event-OR, as well as event-OR and AND, plus hit counting (see section 8 for details) are implemented.

The amount of data to be read via VME sets a lower limit of ~ 2 s for each integration period, well below the initial lower limit to the LB duration actually set by the ATLAS TDAQ and Online Luminosity Calculator systems.

For a quick luminosity information, as needed by LHC for beam monitoring and luminosity levelling, the LUMAT board provides also a few counters of hits and events, evaluated on short intervals of time (down to 0.1 s). The actual integration time is 2 s and counts, suitably converted into luminosity information, are sent to the LHC control room for an immediate feedback on beam settings.

6 Relative calibration system

An important part of producing an accurate luminosity measurement with the new detector is the new calibration system (see figure 18) which is essential to monitor the stability of the photomultipliers gain during a year's running. Three independent calibration systems were designed and built, each exploiting a different principle and applied to a different set of photomultipliers. Initially 16 + 16 PMTs were fed with both LED and LASER light, carried by quartz optical fibers, while 4 + 4 were equipped with ^{207}Bi radioactive sources that produce internal conversion electrons (see section 3.3 for details) above the Cherenkov threshold in the quartz windows (for a pulseheight spectrum see figure 19).

Calibration runs with LED and Bismuth are performed regularly after the end of each LHC fill in order to evaluate gain changes caused by the charge produced inside the dynode chain.
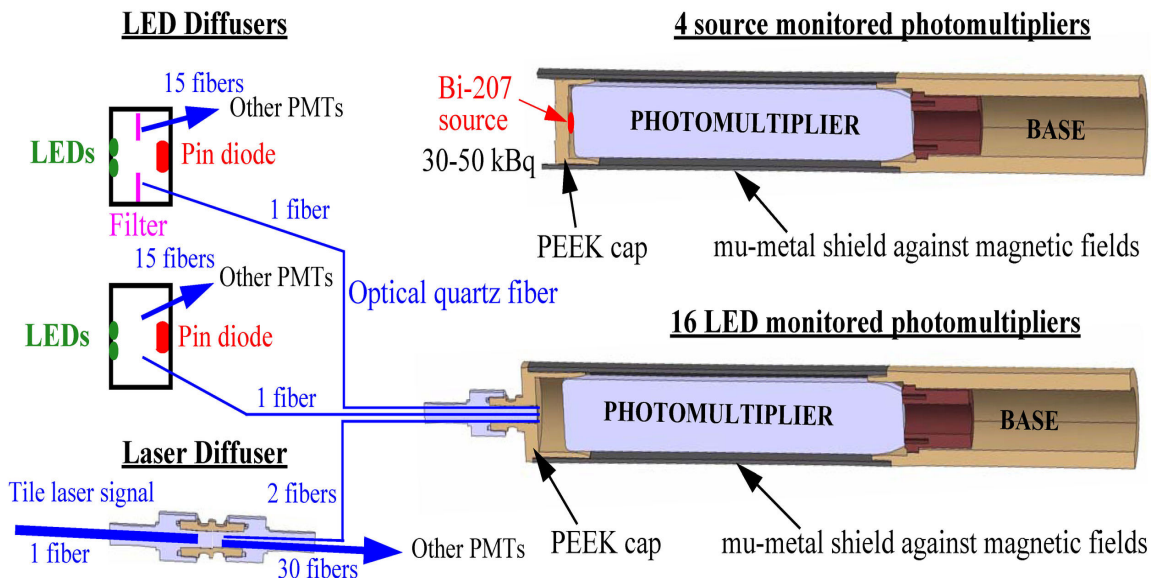

Figure 18. Schematic view of the LUCID-2 relative calibration system for one detector module in 2015.
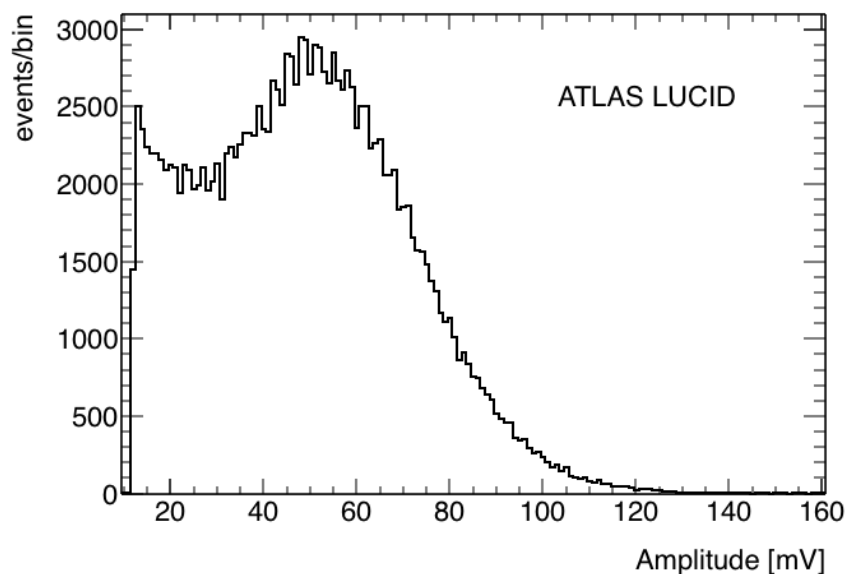
Figure 19. Measurement of the pulseheight distribution of the LUCROD amplified signals from the Bi-source.

6.1 The LED and LASER systems

The LEDs are pulsed at the LHC orbit frequency of about 11 kHz and can produce large signals in the PMTs. The mean value of the amplitude and the charge of the signals collected in calibration runs are used to monitor the gain stability and allow for an automatic correction by changes of the PMT high voltage. The LED intrinsic stability and possible light intensity fluctuations are monitored by PIN-diodes, whose information is therefore used to correct the observed signal in the PMTs. All PMTs are simultaneously illuminated through a special diffuser designed in order to ensure an even light distribution to all PMTs. Due to the smaller sensitivity to the LED light with respect to the PMTs, the PIN-diode is placed directly in front of the LED source, while all PMT calibration fibers surround it in a circle (see figure 20). Another issue related to the different sensitivity of the PIN-diodes and the PMTs is that the LED light must be intense enough for the PIN-diodes, but small enough so the PMT signal do not saturate the readout electronics. For this reason, a ring-shaped filter is placed inside the diffuser in front of the PMT calibration fibers. The produced light is transported to all PMTs via 4.5 meters long, 240 micron diameter quarz fibers. These were tested for radiation damage by irradiation with neutrons and gammas at doses equivalent to those expected after 2 years of LHC exposure [5]. In figure 21 the stability of the LED light is shown as monitored by the PIN-diode. After an initial drop of about 4%, a rather good stability is maintained for the rest of the data taking period during 2016. At the PMT end the LED fibers are connected to the front of the PMTs via fiber connectors that screw on to the PEEK caps (see figures 2 and 4). However during the data-taking it was realized that such connectors are a major source of background, due to activation of the material induced by the large particle fluxes. Such problem is of course absent in the PMTs calibrated with the Bismuth source where the connectors are absent.

A similar approach is also used for the LASER calibration. LASER light is provided by the ATLAS Tile calorimeter calibration system [12] together with a monitoring of the light stability. For this reason no additional monitoring with PIN-diodes is needed. In this case, a diffuser was designed to evenly distribute the light to all PMTs, although a different one due to the fact that the LASER light, contrary to the LED light, is collimated. A cylindrical diffuser connects the single larger fiber coming from the LASER source to a bundle of smaller fibers going to the PMTs, arranged in circular geometry. An air gap in between is dimensioned such as to optimize the light collection and distribution. As the light spot is not radially constant, two fibers for each PMT are used, one in the more central parts of the fiber bundle and one in the peripheral parts so as to optimize the illumination homogeneity among PMTs.
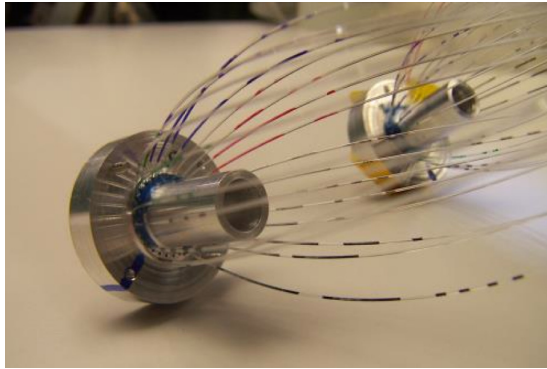

Figure 20. The LUCID LED diffuser. In the center the PIN-diode holder is visible with the PMT calibration fibers surrounding it.
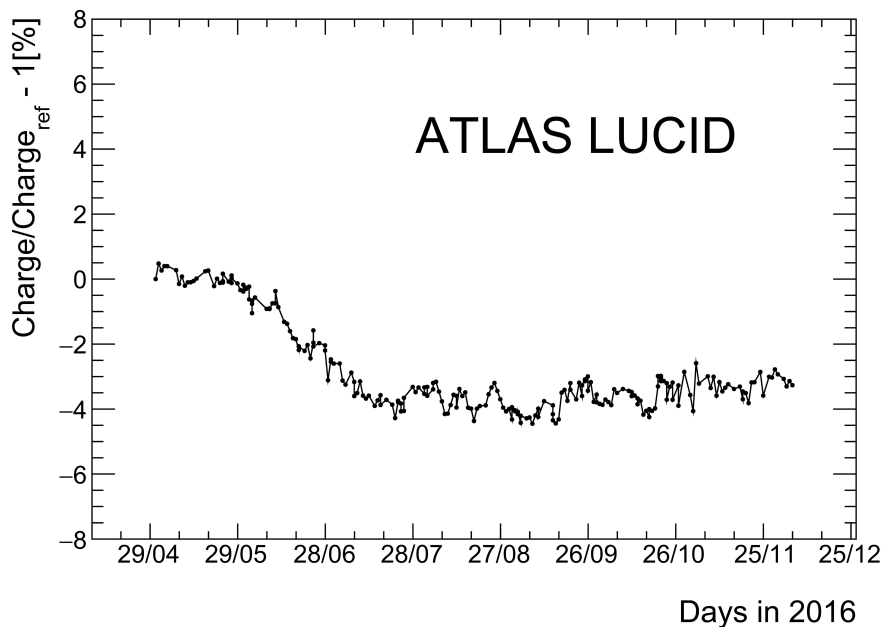

Figure 21. LED calibration signal as monitored by the PIN-diode as a function of time in 2016.

6.2 The ^{207}Bi system

The main reason for using a calibration system based on radioactive sources deposited on the quarz window of the PMTs is that it is intrinsically free from possible instabilities of the input light and from possible degradation of the optical fibers transporting this light due to radiation damage. The wavelength of Cherenkov light is also different from that of LED light which can be important since the efficiency of the photocathodes is wavelength dependent.

A critical parameter to be considered with this method is the activity of the deposited source. This has to be large enough to allow for calibration runs to provide sufficient statistics in a reasonable time, but not too large in order not to interfere with the luminosity measurement during data-taking. The background produced by the Bismuth is in fact present all the time. While this is not an issue during normal high luminosity operation, problems can arise when performing data takings in special conditions, such as the so called van der Meer scans at very low luminosity [13] needed for the absolute luminosity calibration. Indeed, this was one of the main reasons at the beginning for not equipping all PMTs with radioactive sources but keeping LED/LASER-calibrated PMTs as well. A typical activity between 30 and 45 kBq for the various PMTs, corresponding to a dose rate at 3 cm of between 3.5 and 5.5 $\mu Sv/h$ has been used. This activity proved to perfectly meet the two limitations/requirements on efficiency and background.

In order to monitor the gain stability of the photomultipliers, the mean charge and the mean amplitude of signals self-triggered during calibration runs was measured for each photomultiplier. These measurements are used to estimate the PMT gain. In case a deviation is observed with respect to a chosen reference value, an automatic procedure varies the PMT high voltage to compensate for it. This is discussed more in detail below in section 7.

This system was so successful during the 2015 data taking that, as mentioned in section 2, the 4 + 4 photomultipliers in the SPARE sub-detector were replaced with new photomultipliers equipped with ^{207}Bi sources during the 2015–2016 winter shutdown and in the following shutdown the 8 + 8 photomultipliers in the LED and MODIFIED sub-detectors were also exchanged for new ones with ^{207}Bi sources. Starting from the 2017 data taking, only PMTs in the FIBER detector have therefore been calibrated with LED or LASER signals.

7 Operational issues

7.1 PMT High Voltage

The effect of the Bismuth-based relative calibration procedure is shown in figures 22, 23 and 24. In figure 22 the HV applied to the PMTs is plotted as a function of the cumulative luminosity delivered by LHC. The figure shows that the HV was continuously increased during each year, but in the 2016 and 2017 data takings, where larger integrated luminosities were accumulated, a HV plateau was reached where little/no further increases were needed. Moreover the reached HV values are far from the maximum allowed of 1250 Volts.

Integrated luminosity in ATLAS is a quantity that is not easy to relate to other detectors and therefore the integrated charge provided by the photomultipliers and the dose they have been exposed to have also been estimated. The integrated charge in one run was calculated from the

anode current multiplied by the time. Since the anode current is proportional to the luminosity, the conversion factor obtained from one run could be used for the entire data-set.

A set of passive Radio Photo Luminescence (RPL) dosimeters were installed around the LUCID photomultipliers before the start of data taking in 2015 and then a sub-set of these were removed after the data taking and analysed. A dose of 9.4 kGray was measured during a running period that corresponded to 4.2 fb^{-1}. Under the assumption that the accumulated dose is proportional to the integrated luminosity it is possible to estimate the dose for any value of integrated luminosity. The result of the charge and dose measurements are shown in the top scales in figure 22.

In figure 23 the HV increases are shown, separately for the three data taking periods, as a function of the luminosity accumulated in the corresponding year, each set of points being anchored at zero at the beginning of each period. The first important observation is that the slope of the distributions decreases from 2015 to 2017, and the HV increase needed to reach the plateau becomes smaller and smaller (in 2015 the plateau was not reached due to the small delivered luminosity). Finally, the accumulated luminosity at which the plateau starts to show up becomes smaller and smaller. One has to remember that each data taking period is preceded by a few months LHC shutdown, during which the PMTs are not drawing current. The above observations point to the interpretation that, despite each year the PMTs undergo a training period before they eventually stabilize, this period is shorter and shorter and the HV adjustment needed to keep their gain constant becomes smaller and smaller.

The charge deviation relative a reference run as a function of time for the year 2016 is plotted in figure 24 for the bismuth calibration sessions. The figure shows clearly that with the calibration procedure the mean charge was kept constant over the whole running period of several months. It can be seen that after long LHC fills the charge can decrease up to 5%, but is then properly recovered by the HV adjustments.
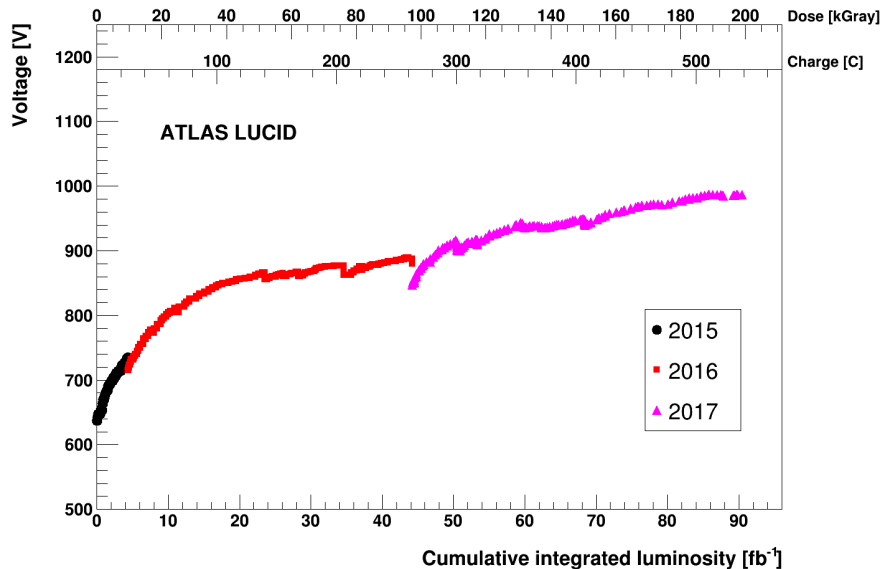

Figure 22. HV applied to the PMTs as a function of cumulative luminosity delivered to the LHC from 2015 to 2017.
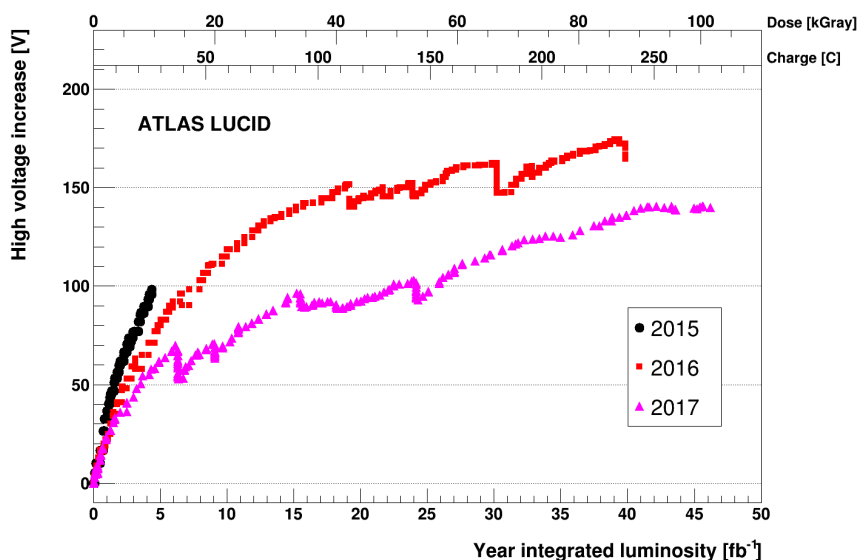
Figure 23. HV applied to the PMTs as a function of integrated luminosity delivered from 2015-2017 for each year separately.
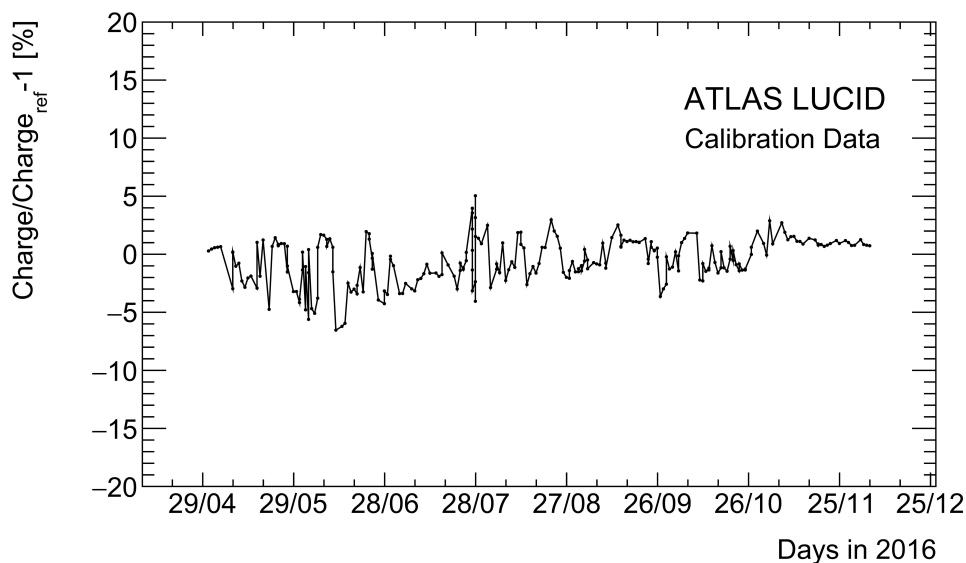
Figure 24. Variation in percent of the measured mean charge relative a reference run for one of the Bi-calibrated photomultipliers.

Up until the last running period in 2015 the gain changed quite slowly and there was enough time to analyse the calibration runs and occasionally increase the high voltage. In the last running period there was a sharp increase in the luminosity which resulted in a fast decrease of the photomultiplier gains. The analysis procedure was then too slow and an automatic script was introduced that calculated the mean charge directly after each calibration run and then used these mean values to correct the high voltage immediately.

This continuous increase of the high voltage had two main consequences:

1) a decrease in the photoelectron transit time within the PMTs, resulting in changes in the signal timing.

2) a change in the signal shape, and in particular in the ratio between signal charge and signal amplitude, which had some measurable effects on the efficiency of some of the luminosity algorithms.

The former effect is shown in figure 25, where the delay of LED signals with respect to a fixed reference time is shown as a function of the applied HV. Since the LED pulser is locked to the orbit signal, any shift in the delay of LED signals closely mimics signals coming from beam collisions. Figure 25 shows that the PMT transit time becomes shorter and shorter as long as the high voltage is increased, eventually reaching a minimum value (the maximum voltage for the PMTs is 1250 V). Due to reasons explained in reference [5], the gain (G) of the PMTs installed in LUCID is set to $G \approx 10^5$, which initially corresponded to an average high voltage of approximately 650 V. At the end of 2016 the high voltage in some PMTs was larger than 850 V, corresponding to a faster PMT transit time than the initial one by more than 10 ns. Such a time shift is 3–4 times the period of the LUCROD digitizer clock, and corresponds to about one half of a BCID period. In order to maintain good performance of the electronics, internal delays of the LUCROD boards had to be continuously adjusted during data taking to compensate for this effect.
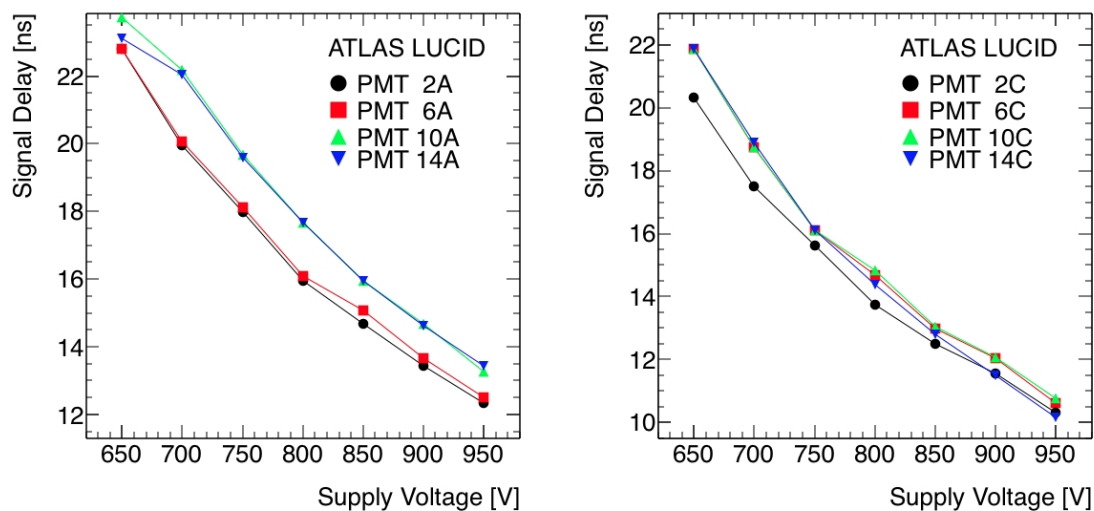
Figure 25. Transit time as a function of HV.

The second effect of the substantial HV change relates to the pulse shape as mentioned above. The effect is summarized in figure 26 in which the ratio of charge over amplitude for the PMT calibration signals is reported as a function of day in the year 2016. In order to keep the PMT gain constant, the HV was increased during the year and this implied a 5% decrease of the ratio of charge over amplitude. A difference in this ratio as a function of HV means that there will be a slight difference in the HV adjustment depending on if one tries to keep the charge or the amplitude

constant. Since the main luminosity algorithms used for LUCID in Run 2 are based on counting the number of times that the amplitude of a signal is above a preset threshold, the parameter to be monitored during the calibration using a ^{207}Bi source is the average of the amplitude.
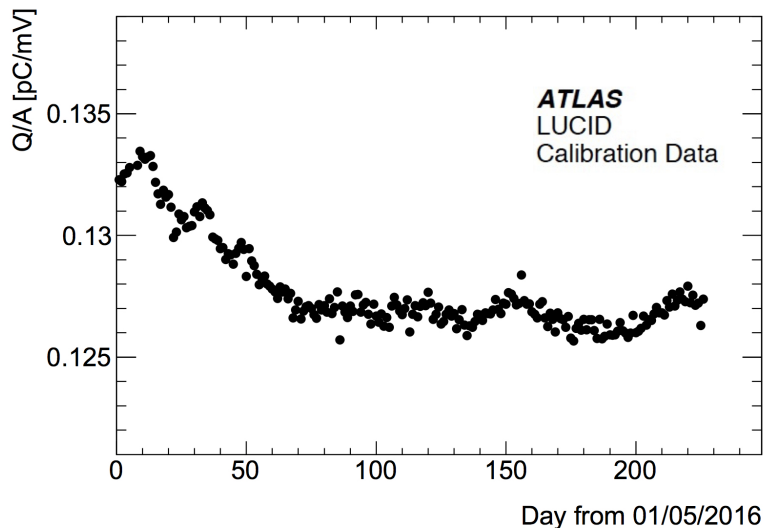

Figure 26. Charge-amplitude ratio as a function of day in 2016.

7.2 Single Event Upset (SEU)

Simulations of the radiation levels in the ATLAS cavern predicted a dose of < 0.1 Gy per year in the location of the LUCROD boards and these boards were not designed to be radiation resistent. However, the firmware in the FPGAs was configured so as to perform cyclic redundancy checks (CRC) at a frequency of about 1 ms. Upon failure of the check, a bit is set that can be detected by software. With ten FPGAs in each LUCROD, and a total of four boards, SEU started to manifest itself with a frequency of about one per week during high luminosity runs since June 2016. The large redundancy and modularity of LUCID data ensured the availability of some good luminosity data in all periods of data taking, but a dedicated recovery procedure had to be implemented to keep the effects of SEU under control.

Since SEU recovery implies reloading of the firmware from flash memory to the affected FPGA, reconfiguration of the latter is also needed. During the recovery time, data in the affected FPGA is not usable. In ATLAS, luminosity counts are related to luminosity block periods, typically lasting between 30 s and 1 minute and a LUCROD SEU recovery is possible with limited data loss since in the worst case two LBs would be lost, should the SEU happen close to LB boundaries.

Failures in the VP917 Single Board Computer (SBC) located in the VME crates hosting the LUCROD boards, probably due to SEU too, occurred once in 2016 and once in 2017. In this case a power cycle of the VME crate was needed to recover, and no data was available for the affected LUCID side for a longer part of the on-going run.

8 The LUCID luminosity measurement

All methods used in ATLAS to measure luminosity are based on the sampling of the rate of inelastic interactions. At a collider where there is rarely more than one interaction for every bunch crossing, the luminosity is proportional to the rate of triggers from a detector that is sensitive to inelastic events. The luminosity at the LHC is, as mentioned before, so high that there are typically many inelastic interactions every time a pair of proton bunches cross each other in ATLAS.

The algorithms used to measure luminosity can be divided up into three groups: event-counting algorithms, hit-counting algorithms and charge integration algorithms. A particular detector and method will in event-counting and hit-counting mode measure a visible number of interactions (μ^{vis}) that depends on the method's efficiency and acceptance (ϵ) to detect a single interaction ($\mu^{\text{vis}} = \epsilon\mu$). The basic principle is to measure μ^{vis} with as high accuracy as possible during a luminosity block and then calculate the average luminosity from:

$$L_{\text{LB}} = \frac{f_{\text{LHC}}}{\sigma_{\text{inel}}} \sum_{j=1}^{n_b} \mu_j = \frac{f_{\text{LHC}}}{\sigma^{\text{vis}}} \sum_{j=1}^{n_b} \mu_j^{\text{vis}} \tag{8.1}$$

where f_{LHC} is the LHC revolution frequency, σ_{inel} is the total inelastic cross section, n_b is the number of bunch pairs colliding in ATLAS and σ^{vis} is the visible cross section, i.e. the inelastic cross section times the efficiency and acceptance of the luminosity method that is being used ($\sigma^{\text{vis}} = \epsilon\sigma_{\text{inel}}$). The problem of measuring luminosity can now be factorized into two parts:

1. Measuring μ^{vis}

2. Absolute calibration, i.e. determining σ^{vis}.

A similar factorization can be done in the case of charge integration.

8.1 Luminosity algorithms

In event-counting algorithms μ^{vis} is determined by measuring the fraction of bunch-crossings in a luminosity block with at least one "event" satisfying some conditions, the simplest of which is the presence of at least one signal above a preset threshold (hit) somewhere in the detector. This is called "Event OR" counting. In "Event AND" counting it is instead required that there is at least one signal in each of the two LUCID detectors on opposite side of the interaction point. Formulas have been derived that relate the measured fractions of OR-events in a luminosity block ($N_{\text{OR}}/N_{\text{BC}}$) to μ^{vis} under the assumption that the number of interactions in a bunch crossing follow a Poissonian distribution [2]:

$$\mu_{\text{vis}}^{\text{OR}} = -\ln\left(1 - \frac{N_{\text{OR}}}{N_{\text{BC}}}\right) \tag{8.2}$$

The Event AND algorithms have the advantage of a lower background and a lower σ^{vis} but there is no simple relationship between μ^{vis} and $N_{\text{AND}}/N_{\text{BC}}$ as described by the formula above. Instead an exponential equation has to be solved numerically [2].

The measured fraction of hits per bunch crossing during a luminosity block ($N_{\text{HIT}}/N_{\text{BC}}/N_{\text{TUBES}}$) are used by the hit-counting algorithms. These algorithms have the advantage of not suffering from zero-starvation even at the highest possible probed μ-values at the LHC but they are more sensitive

to systematic effects than the event counting algorithms. A logarithmic formula similar to the one above can be used to estimate μ^{vis} from $N_{\text{HIT}}/N_{\text{BC}}/N_{\text{TUBES}}$ [2]. With the new LUCID-2 electronics it is also possible to count the number of hits in individual photomultipliers. In this way each photomultiplier can be used as an individual luminosity detector.

The different algorithms mentioned above were employed depending on the μ-range. The μ-value when zero-starvation stops an algorithm from working depends on the length of the luminosity block and the efficiency (σ^{vis}) of the algorithm. For EVENT OR counting with $4 + 4$ PMTs and 60 second long luminosity blocks this happens when $\mu > 34$ while EVENT OR counting with only 4 PMTs (single side OR) have zero starvation when $\mu > 58$. A single side OR algorithm was used as the main luminosity algorithm in 2015 but when the μ-values where increased in 2016 it was necessary to switch to a hit-counting algorithm which have zero starvation only for $\mu > 172$.

The charge algorithms are based on measuring the integral of the photomultiplier pulses and the measured quantity (Q_{TOT}) is the sum of the integrals of all pulses during a luminosity block from either individual photomultipliers or from several photomultipliers. This quantity is proportional to the luminosity and it is not needed to use the logarithmic formula eq. 8.2 above to calculate the luminosity. This is an advantage since eq. 8.2 is derived under the assumption that the number of interactions in a bunch crossing follows a Poissonian distribution and this is not always correct since particles from different pp-interactions in the same bunch crossing can give small signals that when they combine produce a hit. Thus charge algorithms have the advantage that the measured quantity is independent of any statistical assumption. However, those algorithms have the disadvantage of being more sensitive to the background (due to the absence of a threshold as it is in the case of event- or hit-counting algorithms) and to photomultiplier gain changes, which reflect into directly proportional charge variations.

For every algorithm the relevant quantities can be measured both online and offline for individual bunch-crossings. In addition the algorithms can be applied to the standard PMT's with LED or Bi calibration as well as to the modified PMT's and the fiber detectors. An evaluation of the different possible luminosity algorithms requires cross comparison of all different ATLAS luminosity detectors. A future ATLAS luminosity performance paper will include detailed evaluations. Here we will only mention some generalities related to the different algorithms.

8.2 The absolute σ^{vis} calibration

So far the absolute calibration of the various methods has not been discussed. It is done in special fills called van der Meer fills [13] in which the beams are being separated in the horizontal (x) and vertical direction (y) while the interaction rate is being measured with different algorithms. The basic idea is that the luminosity can be obtained from the width of the two scan curves (Σ_x and Σ_y) if the number of colliding protons in the bunches is also measured. One can show that the maximum luminosity for a colliding bunch pair (L^{peak}) can be calculated from the overlap integral of the transverse proton density functions $\rho_1(x, y)$ and $\rho_2(x, y)$ of the two beams 1 and 2 and if these density functions are not correlated in x and y, the integral can be obtained from the scan widths:

$$L^{\text{peak}} = n_{p1}n_{p2}L^{\text{peak}}_{\text{spec}} = f_{\text{LHC}}n_{\text{p1}}n_{\text{p2}} \int \rho_1(x, y)\rho_2(x, y)dxdy = f_{\text{LHC}}n_{\text{p1}}n_{\text{p2}}\frac{1}{2\pi\Sigma_x\Sigma_y} \qquad (8.3)$$

where L_{spec} is the so-called specific luminosity and $n_{\text{p1(2)}}$ is the number of protons in each of the two colliding bunches. It is important to note that the constant background rate from the ^{207}Bi sources is small enough not to spoil the measurement of the width of the scan curve.

For event-counting and hit-counting algorithms σ^{vis} is obtained from the scan widths (Σ_x and Σ_y), the peak μ^{vis} values during the scans and the number of protons ($n_{p1}n_{p2}$) in the colliding bunches. The latter is measured by a pair of DC current transformers (DCCT) that measure the total LHC current and a pair of fast beam current transformers (FBCT) that measure the fraction of the total current in each bunch. The formalism for absolute calibration of the charge algorithms is very similar.

The ATLAS VDM analysis is complicated, with many different systematic uncertainties. It has been described in great detail in previous luminosity notes and papers [2, 14, 15] and will not be presented again in this paper.

9   Conclusions

The operation of the new LUCID-2 detector in LHC run 2 demonstrates that one can build a Cherenkov detector that consists only of photomultipliers with quartz windows. The fact that LUCID-2 has been chosen as the main online and offline luminometer in ATLAS, despite the availability of several other detector systems that can measure the luminosity, shows that this uncomplicated detector concept has been successful. LUCID-2 is at present the only detector available in ATLAS that can measure the luminosity accurately online for each of the up to 2808 colliding bunch pairs in the LHC. These bunch pairs are separated by only 25 ns and new purpose built electronics have been built that can count not only the number of pulses above threshold but also integrate the pulses. The electronics can produce more than 100 luminosity measurements simultaneously and the detector therefore has a lot of redundancy. This is necessary since a luminosity measurement is needed by almost all physics analysis and by some sub-detectors implying that down-times in the luminosity measurement have to be avoided. The operation of the LHC also requires fast and reliable online luminosity measurements from all collision points at all times.

It is well known that the gain of photomultipliers varies with time. The gain goes down when the PMTs are being used and they recover to some extent when they are turned off. The gain of photomultipliers have traditionally been monitored by exposing them to light sources such as LEDs or lasers. The problem with this approach is to keep the light sources stable and one typically needs to also monitor the stability of the light sources. An important part of the LUCID-2 detector is therefore the innovative monitoring system based on radioactive ^{207}Bi sources applied directly to the windows of the photomultipliers. The experience of operating both a LED and a ^{207}Bi system in parallel during Run 2 has shown that the source system provides a significant improvement over the LED system.

By using ^{207}Bi that produces monoenergetic internal conversions electrons above the Cherenkov threshold one produces a signal distribution in the photomultipliers that is very close to that of high-energy particles from the pp-interactions at the LHC. This means that the photomultiplier gain is measured with light of a similar wavelength and intensity and without the use of optical fibers, filters and PIN diodes which can all deteriorate in a harsh radiation environment. The measurement in special monitoring runs of the mean of the amplitude distribution of pulses from ^{207}Bi that are above

a threshold, is also a fast and easy way of monitoring the gain stability. It can be combined with an automatic system that keeps the gain constant by changing the high voltage to the photomultipliers. However the activity of the sources have to be chosen carefully so that it is high enough to give an accurate measurement of the mean amplitude in 10 minute long monitoring runs but not so high that it spoils the very low luminosity measurements in van der Meer scans when the beams are separated.

For the very high luminosity LHC Run 4, the LUCID collaboration is investigating the possibility of building a luminosity detector that uses bundles of optical quartz fibers read-out by photomultipliers in a shielded location. Such a detector has been tested both in LHC Run 1 and 2. The light produced in the fibers is more than enough for an accurate measurement but the amplitude distribution is such that the technique of counting hits will not work. It therefore has to be combined with a charge measurement, i.e. a measurement of the integral of the photomultiplier pulses. The problem is that such a charge measurement is more sensitive to gain variations than a hit measurement and the gain monitoring of such a detector is therefore even more crucial. So far the gain of these photomultiplier has been monitored by injecting LED light onto the windows. This method does not monitor any deterioration of the optical properties of the quartz fibers and so the collaboration is now investigating the possibility of applying ^{207}Bi to quartz discs at the end of the fiber bundles. If this works, a future LUCID-3 detector could be based on bundles of optical quartz fibers monitored by radioactive ^{207}Bi sources.

Acknowledgments

References

[1] ATLAS collaboration, *The ATLAS Experiment at the CERN Large Hadron Collider*, 2008 *JINST* **3** S08003.

[2] ATLAS collaboration, *Luminosity Determination in pp Collisions at $\sqrt{s} = 7$ TeV Using the ATLAS Detector at the LHC*, *Eur. Phys. J.* **C 71** (2011) 1630 [arXiv:1101.2185].

[3] P. Grafström and W. Kozanecki, *Luminosity determination at proton colliders*, *Progr. Part. Nucl. Phys.* **81** (2015) 97.

[4] D. Acosta et al., *The CDF Cherenkov Luminosity Monitor*, *Nucl. Instrum. Meth.* **A 461** (2001) 540.

[5] G.L. Alberghi et al., *Choice and characterization of photomultipliers for the new ATLAS LUCID detector*, 2016 *JINST* **11** P05014.

[6] T. Sjöstrand, S. Mrenna and P.Z. Skands, *PYTHIA 6.4 Physics and Manual*, *JHEP* **05** (2006) 026 [hep-ph/0603175].

[7] GEANT4 collaboration, S. Agostinelli et al., *GEANT4: A Simulation toolkit*, *Nucl. Instrum. Meth.* **A 506** (2003) 250.

[8] R. Engel, *Photoproduction within the two component dual parton model. 1. Amplitudes and cross-sections*, *Z. Phys.* **C 66** (1995) 203;
R. Engel and J. Ranft, *Hadronic photon-photon interactions at high-energies*, *Phys. Rev.* **D 54** (1996) 4244 [hep-ph/9509373].

[9] C. Zeitnitz and T.A. Gabriel, *The GEANT - CALOR interface and benchmark calculations of ZEUS test calorimeters*, *Nucl. Instrum. Meth.* **A 349** (1994) 106.

[10] A. Annovi et al., *The EDRO Board Connected to the Associative Memory: a "Baby" FastTracKer Processor for the ATLAS Experiment*, *Phys. Procedia* **37** (2012) 1772.

[11] ATLAS collaboration, ATLAS HLT/DAQ/DCS Group, *ATLAS high-level trigger, data-acquisition and controls: Technical Design Report*, ATLAS-TDR-016, [CERN-LHCC-2003-022].

[12] ATLAS Tile Calorimeter group, *The Laser calibration of the ATLAS Tile Calorimeter during the LHC run 1*, 2016 *JINST* **11** T10005 [arXiv:1608.02791].

[13] S. van der Meer, *Calibration of the effective beam height in the ISR*, CERN-ISR-PO-68-31 (1968).

[14] ATLAS collaboration, *Improved luminosity determination in pp collisions at $\sqrt{s} = 7\,TeV$ using the ATLAS detector at the LHC*, *Eur. Phys. J.* **C 73** (2013) 2518 [arXiv:1302.4393].

[15] ATLAS collaboration, *Luminosity determination in pp collisions at $\sqrt{s} = 8\,TeV$ using the ATLAS detector at the LHC*, *Eur. Phys. J.* **C 76** (2016) 653 [arXiv:1608.03953].